The British Journal of Radiology, 84 (2011), 271–278

Clinical target volume delineation in glioblastomas: pre-operative versus post-operative/pre-radiotherapy MRI

[1]P FARACE, PhD, [2]M G GIRI, [2]G MELIADÒ, [3]D AMELIO, MD, [3]L WIDESOTT, [4]G K RICCIARDI, MD, [5]S DALL'OGLIO, MD, [2]A RIZZOTTI, [1]A SBARBATI, MD, [4]A BELTRAMELLO, MD, [5]S MALUTA, MD and [3]M AMICHETTI, MD

[1]*Department of Morphological-Biomedical Sciences, Section of Anatomy and Histology, University of Verona, Italy,* [2]*Medical Physics Department, Borgo Trento Hospital, Verona, Italy,* [3]*ATreP, Provincial Agency for Protontherapy, Trento, Italy,* [4]*Neuroradiology Department, Borgo Trento Hospital, Verona, Italy and* [5]*Radiotherapy Department, Borgo Trento Hospital, Verona, Italy*

Objectives: Delineation of clinical target volume (CTV) is still controversial in glioblastomas. In order to assess the differences in volume and shape of the radiotherapy target, the use of pre-operative *vs* post-operative/pre-radiotherapy T_1 and T_2 weighted MRI was compared.

Methods: 4 CTVs were delineated in 24 patients pre-operatively and post-operatively using T_1 contrast-enhanced ($T1_{PRE}$CTV and $T1_{POST}$CTV) and T_2 weighted images ($T2_{PRE}$CTV and $T2_{POST}$CTV). Pre-operative MRI examinations were performed the day before surgery, whereas post-operative examinations were acquired 1 month after surgery and before chemoradiation. A concordance index (CI) was defined as the ratio between the overlapping and composite volumes.

Results: The volumes of $T1_{PRE}$CTV and $T1_{POST}$CTV were not statistically different (248 ± 88 *vs* 254 ± 101), although volume differences >100 cm^3 were observed in 6 out of 24 patients. A marked increase due to tumour progression was shown in three patients. Three patients showed a decrease because of a reduced mass effect. A significant reduction occurred between pre-operative and post-operative T_2 volumes (139 ± 68 *vs* 78 ± 59). Lack of concordance was observed between $T1_{PRE}$CTV and $T1_{POST}$CTV ($CI=0.67 \pm 0.09$), $T2_{PRE}$CTV and $T2_{POST}$CTV ($CI=0.39 \pm 0.20$) and comparing the portion of the $T1_{PRE}$CTV and $T1_{POST}$CTV not covered by that defined on $T2_{PRE}$CTV images ($CI=0.45 \pm 0.16$ and 0.44 ± 0.17, respectively).

Conclusion: Using T_2 MRI, huge variations can be observed in peritumoural oedema, which are probably due to steroid treatment. Using T_1 MRI, brain shifts after surgery and possible progressive enhancing lesions produce substantial differences in CTVs. Our data support the use of post-operative/pre-radiotherapy T_1 weighted MRI for planning purposes.

Received 11 June 2009
Revised 8 January 2010
Accepted 27 January 2010

DOI: 10.1259/bjr/10315979

The current standard of care for newly diagnosed glioblastoma (GBM) is maximal surgical debulking, followed by adjuvant radiation therapy (RT) and temozolomide chemotherapy [1]. Although RT has been a standard post-operative treatment for GBM for more than 25 years [2], it is under continuous investigation [3], and there are some controversies about the optimal way to deliver this therapy [4].

Radiation treatment volume is one of these incompletely studied issues, even if the use of CT and MRI has greatly improved the accuracy and reproducibility of tumour localisation and delineation. Some established national guidelines [5, 6] have been suggested; however, currently, there is no consensus on what volume constitutes the optimal RT target. Also, in current glioblastoma trial protocols (*e.g.* the Radiation Therapy Oncology Group (RTOG) 0825 phase III trial [7] and European Organization for Research and Treatment of Cancer (EORTC) 26082–22081 [8]), a different use of T_1/T_2 MRI scans acquired pre- or post-operatively has been suggested.

There are several data showing that the natural history of GBM has a tendency for local recurrence, with complete resection being virtually impossible because of the infiltrative nature of this disease. More than 80% of recurrences occur within 2 cm of the original tumour margin [9–12], even after complete macroscopic resection. These data support the generally accepted practice of delivering external beam RT on the target defined by conventional contrast-enhanced MRI (or CT). In this approach, the gross tumour volume (GTV) includes the contrast-enhancing lesion seen on pre-operative examination or, alternatively, the cavity and residual enhancing lesion on post-operative images. Then a uniform margin, of approximately 2.0 cm, is usually added to address clinically occult glioma cells and to create the clinical target volume (CTV). Alternatively, the perifocal oedema visible at the pre-operative scan, with [11] or without [10] an additional margin of approximately 2 cm, has been investigated as the CTV.

Address correspondence to: Paolo Farace, Department of Morphological and Biomedical Sciences, Anatomy and Histology Section, University of Verona, Via Le Grazie, 8, 37134 Verona (VR), Italy. E-mail: paolofarace@anatomy.univr.it

Since target volume delineation can translate into improved tumour control and/or reduced radiation toxicity, any effort should be made to identify the optimal imaging approach. Nevertheless, the application of limited radiation fields needs safety margins: a 2 cm GTV expansion is considered a good compromise to irradiate about 85% of tumour cells and to simultaneously spare healthy tissues [13]. The irradiation of normal brain can determine atrophy and may result in late sequelae as cognitive deficits, progressive global dementia, apathy and personality changes [14–16]. These clinical findings are consistent with extensive radiation-related damage to brain tissues reported in histological studies [17]. An increase in oedema indicates an alteration in vascular permeability whereas loss of myelin, vascular changes and necrosis are associated with delayed reactions [18]. Radiation injury and severe clinical symptoms depend on the irradiated volume and other radiation parameters such as total delivered dose, fraction size and treatment duration [19].

Herein, in order to assess possible differences in volume and shape of the radiotherapy target, which can result in target missing and/or differences in the amount of normal tissue irradiated, the use of pre-operative *vs* post-operative/pre-radiotherapy T_1 and T_2 weighted MRI were compared. For this purpose, three widely proposed volumes for the delineation of the radiotherapy target in patients affected by GBM were compared: (1) the enhancing volume delineated on T_1 weighted pre-operative MRI scans plus 2 cm of margin; (2) the resection cavity and residual enhancing area plus 2 cm on post-operative MRI examinations; and (3) the oedema identified on pre-operative T_2 weighted images. A further CTV was delineated post-operatively on the T_2 weighted images.

Methods and materials

Participants and study design

The MRI examinations of 24 patients (16 males and 8 females) with intracranial GBM (confirmed at histopathological examination) were analysed. All the patients had surgical debulking using craniotomy. For surgical planning and monitoring purposes, MRI examinations were performed the day before surgery, and 31 $\pm$ 3 days (range 26–36) after surgery, before the beginning of adjuvant chemoradiation. After MR images registration, three CTVs were delineated: pre- and post-operatively on T_1 contrast-enhanced images, and pre-operatively on T_2 weighted images, as defined in detail in the image analysis section.

In order to evaluate changes after surgery owing to steroid administration and tumour removal, a further CTV was delineated post-operatively on the T_2 weighted images.

MR acquisitions

The day before surgical resection, the multimodal MR examination included contrast-enhanced (gadolinium-diethylenetriamine penta-acetic acid (Gd-DTPA)) T_1 weighted imaging by multislice spin echo sequence (repetition time (TR), 500 ms; echo time (TE), 11 ms; slices 20, axial; slice thickness, 5 mm; field of view, 240 $\times$ 240 mm; matrix, 256 $\times$ 256; average, 1) acquired at 3.0 T. A further T_2 examination was performed by a fluid attenuated inversion recovery (FLAIR) sequence (TR, 9000 ms; TE, 100 ms; number of social slices, 20; slice thickness, 5 mm; field of view, 240 $\times$ 240 mm; matrix, 256 $\times$ 256; average, 1).

1 month post-operatively, the MRI examination was repeated including both the T_1 weighted contrast-enhanced images and the T_2 weighted images acquired before surgery.

Image analysis

MR images were transferred to a commercial treatment planning system (Eclipse, Varian Medical Systems Palo Alto, CA), where they were matched together using the available tools for image co-registration. Image registration was performed by an automatic mutual information algorithm or, when the results were not considered satisfactory after visual inspection, by means of 5–9 matching points on anatomical landmarks. Visual inspection gave major relevance to the region surrounding the lesions. The procedure was repeated, adding or moving landmarks, to improve the quality of registration. Tumour volumes were drawn independently by two physicians (MA and DA). The two contours were then simultaneously displayed and visually evaluated by the two physicians and revised by a neuroradiologist (GKR) to resolve any incongruence and to obtain the definitive contour.

In detail, a GTV was delineated as the whole enhancing portion in the pre-operative images ($T1_{PRE}GTV$), and the resection cavity plus (if any) enhancing residual tumour in the post-operative examination ($T1_{POST}GTV$). The corresponding $T1_{PRE}CTV$ and $T1_{POST}CTV$ were obtained by adding a 2.0 cm automatically expanded uniform margin to the corresponding GTVs. The obtained CTVs were then manually reduced in the vicinity of anatomical barriers for tumour spread (*i.e.* skull, tentorium, falx cerebri).

Furthermore, to draw $T2_{PRE}CTV$ and $T2_{POST}CTV$, the area of high signal intensity was delineated on T_2 weighted pre- and post-operative images, without adding any margin.

The differently delineated volumes were calculated in each patient, and compared with each other by paired Student's *t*-test.

To further compare two differently delineated CTVs (CTV_I and CTV_{II}), the overlapping volumes ($CTV_I \cap CTV_{II}$) and the composite volumes ($CTV_I \cup CTV_{II}$) were calculated (Figure 1) by the treatment planning system, and a concordance index (CI) was defined as the ratio between the overlap and composite volumes according to the following equation:

$$CI = (CTV_I \cap CTV_{II})/(CTV_I \cup CTV_{II})$$

Higher scores of CI mean better concordance between the two considered CTVs; low scores of CI mean worse

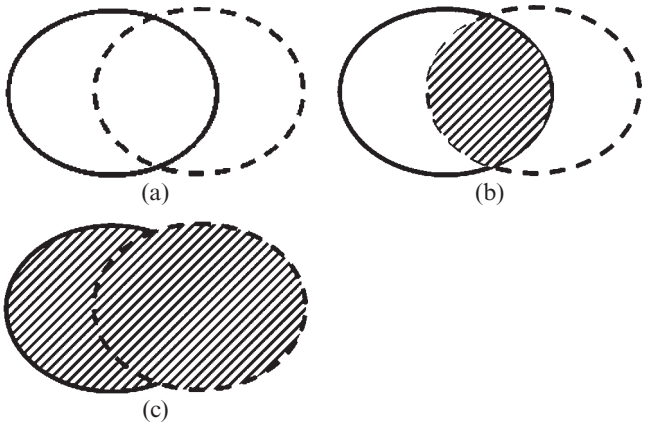

Figure 1. To compare two differently delineated volumes (a), represented by continuous and dashed lines respectively, the overlapping volume (b) and the composite volume (c) were calculated.

concordance and, therefore, a markedly different irradiation of tumour and brain volumes.

Finally, a discordance clinical target volume D_{CTV} defined as:

$$D_{CTV}(\text{I vs II}) = CTV_I - (CTV_I \cap CTV_{II})$$

was used to identify the volume of CTV_I not covered by CTV_{II}.

Assessment of tumour progression before radiotherapy

When a large CTV increase was measured between pre-operative and post-operative/pre-radiotherapy T_1 contrast-enhanced images, the early post-operative T_1 MR examination performed within 48 h after surgery was retrospectively evaluated to better assess the increased extent of blood–brain barrier leakage. A contrast-enhanced (Gd-DTPA) multislice spin echo sequence had been acquired at 1.0 T (TR, 600 ms; TE, 11 ms; number of axial slices, 20 slice thickness, 5 mm; field of view, 220 × 220 mm; matrix, 256 × 256; average, 1).

Results

Target volumes

The mean values of the delineated volumes are shown in Table 1. The CTVs (and the corresponding GTVs) calculated on T_1 pre-operative images were not significantly (at a 0.05 level) different from those calculated on T_1 post-operative images. However, volume changes larger than 30 cm^3 were observed between pre-operative and post-operative GTVs. Accordingly, comparing $T1_{PRE}$CTV with $T1_{POST}$CTV (Figure 2), volume differences >100 cm^3 were observed in 6 out of 24 (25%) patients: a marked volume increase owing to tumour progression in 3 out of 24 (12.5%) patients (patients 1, 6 and 14) and a marked volume decrease owing to reduced mass effect in 3 out of 24 (12.5%) patients (patients 2, 8 and 23).

In Figure 3, the increased extent of blood–brain barrier leakage observed in patient 14 is shown; the MR examination performed within 48 h after surgery enabled better assessment of tumour progression.

Both $T1_{PRE}$CTV and $T1_{POST}$CTV were significantly higher than $T2_{PRE}$CTV ($p < 0.05$). Because a significant reduction in the volume of oedema occurred post-operatively, $T2_{POST}$CTV was significantly ($p < 0.05$) lower than $T2_{PRE}$CTV.

Figure 4 shows how CTVs were defined and shows an example (patient 8) with marked differences among the volumes delineated because of a reduced mass effect.

Overlapping and discordance volumes

The overlapping volumes (Table 1) showed incomplete concordance between $T1_{PRE}$CTV and $T1_{POST}$CTV. Furthermore, comparing the overlapping volumes $T1_{PRE}$CTV ∩ $T2_{PRE}$CTV and $T1_{POST}$CTV ∩ $T2_{PRE}$CTV with the whole $T2_{PRE}$CTV (122 and 118 *vs* 139 cm^3), it appeared that more than 80% of the $T2_{PRE}$CTV was covered by the CTVs delineated on T_1 images. The overlapping CTVs are shown in Figure 2 and their comparison with the CTVs identifies the D_{CTV}. Large $T2_{PRE}$CTVs, which were not covered by the two CTVs delineated at T_1 images, occurred only in patients 5 and 11. A larger D_{CTV} was observed when comparing the portion of the CTV defined on T_1 images that

Table 1. Delineated volumes, overlapping clinical target volume and concordance indexes

	MR images	Mean ± SD	Range
Gross tumour	$T1_{PRE}$GTV	37 ± 26	2–94
Volume (cm^3)	$T1_{POST}$GTV	39 ± 39	7–178
CTV (cm^3)	$T1_{PRE}$CTV	248 ± 88	97–473
	$T1_{POST}$CTV	254 ± 101	138–501
	$T2_{PRE}$CTV	139 ± 68	24–254
	$T2_{POST}$CTV	78 ± 59	15–236
Overlapping CTVs (cm^3)	$T1_{PRE} \cap T1_{POST}$	202 ± 73	92–353
	$T2_{PRE} \cap T2_{POST}$	61 ± 44	3–153
	$T1_{PRE} \cap T2_{PRE}$	122 ± 59	24–219
	$T1_{POST} \cap T2_{PRE}$	118 ± 54	24–196
Concordance index (CTVs)	$T1_{PRE}$ *vs* $T1_{POST}$	0.67 ± 0.09	0.52–0.88
	$T2_{PRE}$ *vs* $T2_{POST}$	0.39 ± 0.20	0.09–0.75
	$T1_{PRE}$ *vs* $T2_{PRE}$	0.45 ± 0.16	0.15–0.73
	$T1_{POST}$ *vs* $T2_{PRE}$	0.44 ± 0.17	0.14–0.73
Concordance index (GTVs)	$T1_{PRE}$ *vs* $T1_{POST}$	0.37 ± 0.15	0.08–0.60

GTV, gross target volume; CTV, clinical target volume; SD, standard deviation.

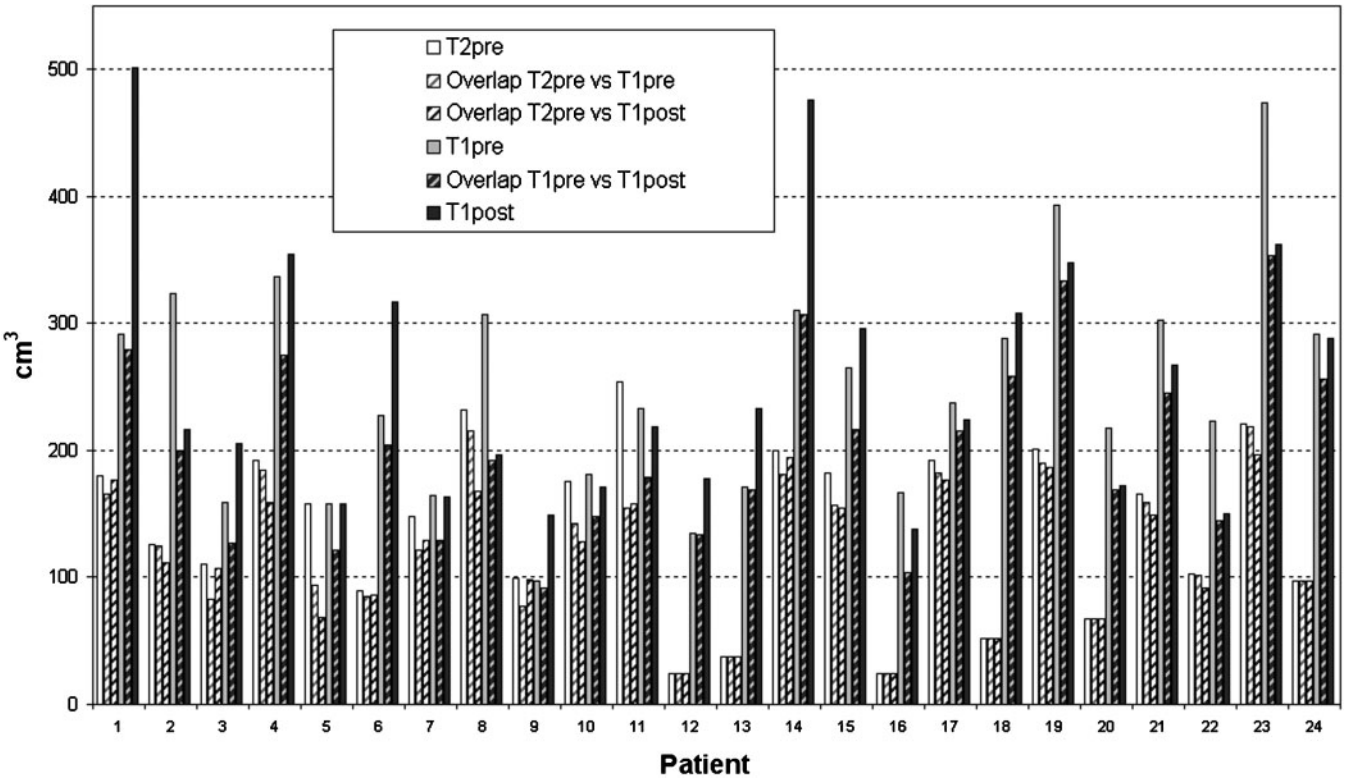

Figure 2. Clinical target volumes (CTV) (in cm^3) and the respective overlapping volumes in each patient examined by $T1_{PRE}$, $T1_{POST}$ and $T2_{PRE}$ scans. For every pair of examinations, the volume of CTV_I not covered by CTV_{II}, *i.e.* the discordance clinical target volume D_{CTV}, can be easily extrapolated.

was not covered by that defined on $T2_{PRE}$ images. The mean volume of $T1_{POST}$CTV not covered by $T1_{PRE}$CTV, *i.e.* $D_{CTV}(T1_{POST}$ *vs* $T1_{PRE})$, was 52 ± 53 cm^3 and the corresponding brain volume covered by $T1_{PRE}$CTV but outside $T1_{POST}$CTV, *i.e.* $D_{CTV}(T1_{PRE}$ *vs* $T1_{POST})$, was 46 ± 36 cm^3. In patient 2, more than 120 cm^3 of brain tissue that was not included in the $T1_{POST}$CTV was included in the $T1_{PRE}$CTV; in patient 14, a substantial incomplete (about 170 cm^3) coverage of the more reliable $T1_{POST}$CTV occurred; in patient 11, both a potential missing of the target (about 40 cm^3) and brain irradiation (about 55 cm^3) would occur if the $T1_{PRE}$CTV was used instead of the $T1_{POST}$CTV as the target.

Concordance indexes

Comparing pre- and post-operative T_1 volumes, the CI values increased from the GTVs to the CTVs as an effect of the isotropic 2.0 cm expansion (Table 1). However, even this higher CI showed that marked changes occurred between the pre-operative and the post-operative scans. The low CIs obtained by using $T2_{PRE}$CTV were the result of the substantial changes in the amount of oedema after surgery (comparing $T2_{PRE}$CTV *vs* $T2_{POST}$CTV) and of the smaller volume of $T2_{PRE}$CTV with respect to the two CTVs delineated on the T_1 images ($T1_{PRE}$CTV *vs* $T2_{PRE}$CTV, and $T1_{POST}$CTV vs $T2_{PRE}$CTV).

Discussion

Delineation of CTV in the planning of post-operative irradiation of GBM is controversial, producing non-uniform CTV sizes and RT fields. As a consequence, target volumes can change considerably according to different treatment guidelines.

The macroscopic extension of GBM tumour is usually identified with the whole enhancing portion on the pre-operative images, or with the resection cavity plus the possible enhancing residual tumour on the post-operative examination. On the other hand, the delineation of the CTV, *i.e.* of the microscopic tumour extension, is an unresolved issue, since the spread of tumour cells in the infiltrating and not enhancing portion is poorly detectable by the clinical imaging methods currently available.

Simple MRI techniques, such as those used in our study, are inadequate for precise volume delineation in GBM, but other imaging techniques using MR or radiotracers [20, 21] have been able to identify the metabolically active tumour tissues within the anatomical region of interest and could be used in clinical routine. Advanced MR approaches, such as spectroscopy and diffusion tensor imaging, resulted in a better correlation with histopathological findings [22–24] and the pattern of recurrence during follow-up [25–27]. Furthermore, data of biopsy specimens of infiltrating tumour tissue showed promising sensitivity and specificity of ^{11}C-methionine positron emission tomography [28], which also appeared able to identify areas at high risk of recurrence [29]. However, these advanced methods are not yet completely established and further investigations are warranted before their acceptance as guidelines in clinical practice. A thorough and complete discussion of the use of new biological functional imaging methods for more accurate target delineation is beyond the scope of this paper.

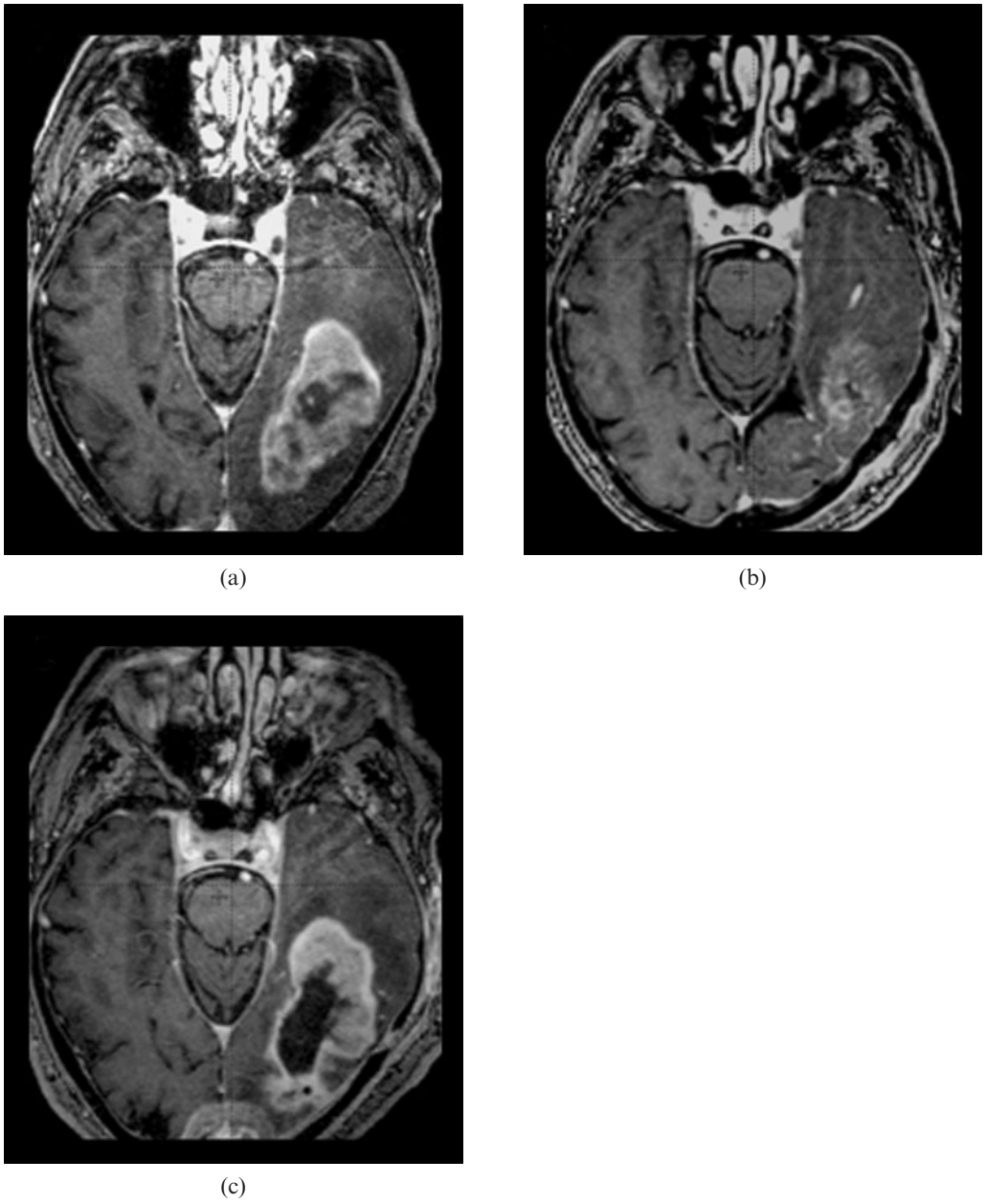

Figure 3. Increased extent of blood–brain barrier leakage observed in patient 14. The contrast-enhancing tumour portion, which is visible on the pre-operative MRI (a), was reduced by surgical resection, as confirmed by early post-operative MRI (b) that was performed within 48 h after surgery. Tumour progression occurred during the time that elapsed before the beginning of radiotherapy, with an enlargement of the contrast-enhancing volume in the pre-radiotherapy images (c), which produced a $T1_{POST}$CTV larger than the $T1_{PRE}$CTV.

Currently, in clinical practice, only conventional CT/MRI methods are routinely applied, on the basis of their proven correlation with the histopathological observation and/or with the pattern of recurrence. Ante- or post-mortem CT/MRI compared with ante- or post-mortem pathological observations in patients with untreated high-grade glioma have shown macro- and microscopic tumour extension within a 2 cm margin of the original visualised mass [13]. Furthermore, the recurrence patterns after irradiation, documented by CT/MRI, have shown that more than 90% of the tumours recur within a 2 cm margin of the primary site [9–12]. To date, on the basis of these findings, the prevalent approach is to define the CTV as the GTV plus an additional margin of 2–3 cm, which can be reduced in the vicinity of anatomical barriers for tumour spread.

Alternatively, the perifocal oedema is proposed as the CTV, since it has been supposed to contain infiltrating tumour cells [30, 31]. However, analysis of the recurrence patterns showed that the complete irradiation of perifocal oedema (with [11] or without [10] expansion) was not found to be necessary. Moreover, peritumoural oedema did not accurately correlate with the presence of tumour cells detected at histological examination [32, 33]. These data suggest that peritumoural oedema merely coexists with infiltrating tumour cells, and that it may simply represent the result of mass effect and of tumour-secreted vascular permeability factors. Accordingly, our

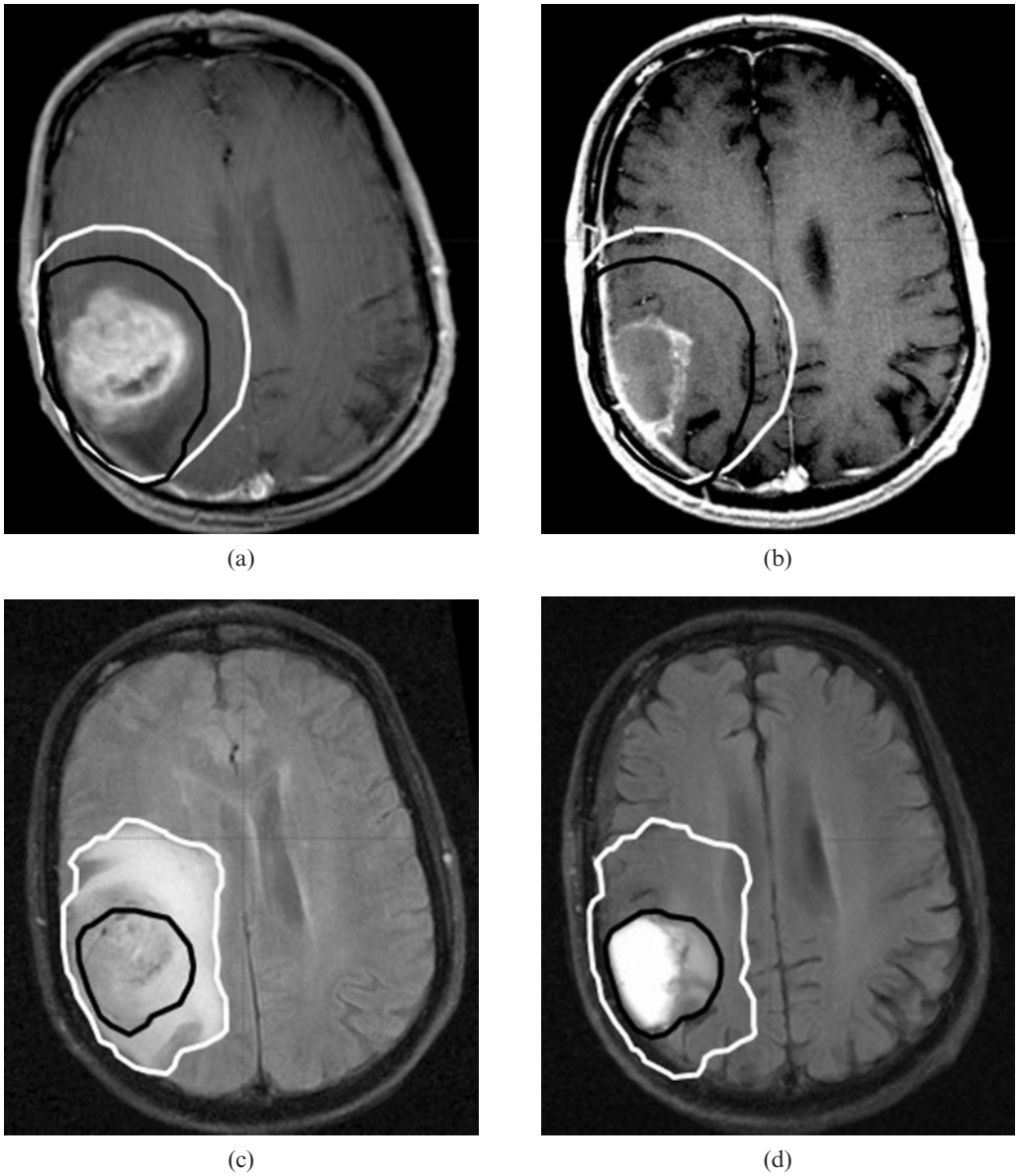

Figure 4. Pre-operative (white line) and pre-radiotherapy (black line) Clinical target volumes (CTV) contours of patient 8. Representative sections of T_1 pre-operative (a), T_1 pre-radiotherapy (b), T_2 pre-operative (c) and T_2 pre-radiotherapy (d) show a decrease in CTV because of the reduced mass effect and reduced oedema.

data showed a significant decrease in the volume of oedema between pre-operative and post-operative T_2 MRIs. Since this was presumably due to gross tumour removal and steroid treatment, our data confirm that factors other than the presence of infiltrating tumour cells determine the extension of peritumoural oedema.

The proximity to the GTV is a widely accepted factor in predicting the initial site of recurrences, but the use of contrast-enhanced T_1 MRI for its delineation is not yet standardised. The pre-operative examination, needed for planning surgical treatment, is routinely used in many countries to also plan radiation therapy. The acquisition of a post-operative contrast-enhanced scan performed within 48 h has been recommended [5], in order to differentiate between enhancing residual tumour and post-operative changes. However, several problems limit the possibility of undertaking these scans within 48 h: physical difficulties in the initial post-operative period (neurological disabilities, wound healing, etc.), limited ability to adopt an adequate set-up during the examination and trouble in using the immobilisation casts, and scheduling problems since the referral for radiotherapy is frequently done only after the histopathological confirmation of disease.

Even in the literature regarding the pattern of recurrence, the correlation between follow-up analysis and expanded GTV was reported using both pre-operative [10, 12] and post-operative/pre-radiotherapy [9, 11] examinations.

Our data clearly show that the two methods can result in different treatment volumes. Despite there being no significant differences observed when comparing $T1_{PRE}$CTV with $T1_{POST}$CTV volumes, substantial differences were observed as a result of tumour displacement after surgery or tumour progression. The reduction in the mass effect after surgery can produce brain shifts,

which could significantly affect the dose distribution if it is planned on pre-surgical examinations. In our data, the average brain area of 46 cm^3 could be within the $T1_{PRE}$CTV, but outside the $T1_{POST}$CTV. As a consequence, planning the radiotherapy based on the $T1_{PRE}$CTV could potentially irradiate large brain volumes at full dosage that are not included in the $T1_{POST}$CTV.

Furthermore, since tumour progression in GBM was observed both after surgery [34] and during RT [35], it is difficult to determine the most appropriate time for baseline RT imaging. Comparing $T1_{PRE}$GTV with $T1_{POST}$GTV, our data showed a markedly larger enhancing volume in 3 out of 24 patients. This suggests that true tumour progression occurs during the time elapsed between surgery and the beginning of adjuvant therapy. Thus, the use of $T1_{PRE}$CTV could produce an incomplete coverage of the tumour volume $T1_{POST}$CTV.

Conclusions

As supported by our data, the delineated CTV depends on the MRI sequences used (T_2 *vs* T_1) and times of acquisition (pre- *vs* post-operative). Relevant spatial and volumetric differences occurred in 25% of the 24 patients analysed.

To plan radiotherapy, a post-operative contrast-enhanced T_1 MR examination performed before the beginning of adjuvant chemoradiation should be preferred to pre-operative data. This provides a more reliable way to delineate the "adapted" CTV. The availability of a post-operative/pre-radiotherapy MRI examination allows consideration of brain shift after surgery and a proper assessment of the tumour status before adjuvant treatment. Such assessment provides a better baseline for an adequate follow-up.

References

1. Stupp R, Hegi ME, Gilbert MR, Chakravarti A. Chemoradiotherapy in malignant glioma: standard of care and future directions. J Clin Oncol 2007;25:4127–36.
2. Laperriere N, Zuraw L, Cairncross G. Cancer Care Ontario Practice Guidelines Initiative Neuro-Oncology Disease Site Group. Radiotherapy for newly diagnosed malignant glioma in adults: a systematic review. Radiother Oncol 2002;64: 259–73.
3. Baumert BG, Brada M, Bernier J, Kortmann RD, Dehing-Oberije C, Collette L, et al. EORTC 22972–26991/MRC BR10 trial: fractionated stereotactic boost following conventional radiotherapy of high grade gliomas. Clinical and quality-assurance results of the stereotactic boost arm. Radiother Oncol 2008;88:163–72.
4. Buatti J, Ryken TC, Smith MC, Sneed P, Suh JH, Mehta M, et al. Radiation therapy of pathologically confirmed newly diagnosed glioblastoma in adults. J Neurooncol 2008;89: 313–37.
5. Mason WP, Maestro RD, Eisenstat D, Forsyth P, Fulton D, Laperrière N, et al. Canadian recommendations for the treatment of glioblastoma multiforme. Curr Oncol 2007;14: 110–17.
6. Frappaz D, Chinot O, Bataillard A, Ben Hassel M, Capelle L, Chanalet S, et al. Summary version of the standards, options and recommendations for the management of adult patients with intracranial glioma. Br J Cancer 2003;89: S73–83.
7. RTOG 0825. Available from: http://www.rtog.org/members/active.html#brain.
8. EORTC protocol 26082–22081. Available from: www.eortc.be/protoc/listprot.asp?kind=group&grp=1.
9. Chan JL, Lee SW, Fraass BA, Normolle DP, Greenberg HS, Junck LR, et al. Survival and failure patterns of high-grade gliomas after three-dimensional conformal radiotherapy. J Clin Oncol 2002;20:1635–42.
10. Aydin H, Sillenberg I, von Lieven H. Patterns of failure following CT-based 3-D irradiation for malignant glioma. Strahlenther Onkol 2001;177:424–31.
11. Chang EL, Akyurek S, Avalos T, Rebueno N, Spicer C, Garcia J, et al. Evaluation of peritumoral edema in the delineation of radiotherapy clinical target volumes for glioblastoma. Int J Radiat Oncol Biol Phys 2007;68:144–50.
12. Oppitz U, Maessen D, Zunterer H, Richter S, Flentje M. 3D-recurrence-patterns of glioblastomas after CT-planned postoperative irradiation. Radiother Oncol 1999;53:53–7.
13. Hochberg FH, Pruitt A. Assumptions in the radiotherapy of glioblastoma. Neurology 1980;30:907–11.
14. Duchstein S, Gademann G, Peters B. Early and late effects of local high dose radiotherapy of the brain on memory and attention. Strahlenther Onkol 2003;179:441–51.
15. Archibald YM, Lunn D, Ruttan LA, Macdonald DR, Del Maestro RF, Barr HW, et al. Cognitive functioning in long-term survivors of high grade glioma. J Neurosurg 1994;80: 247–253.
16. Bosma I, Vos MJ, Heimans JJ, Taphoorn MJ, Aaronson NK, Postma TJ, et al. The course of neurocognitive functioning in high-grade glioma patients. Neuro Oncol 2007;9:53–62.
17. Valk PE, Dillon WP. Radiation injury of the brain. AJNR Am J Neuroradiol 1991;12:45–62.
18. Burger PC, Mahaley MS, Dudka L, Vogel FS. The morphologic effects of radiation administered therapeutically for intracranial gliomas: a post-mortem study of 25 cases. Cancer 1979;44:1256–72.
19. Steen RG, Spence D, Wu S, Xiong X, Kun LE, Merchant TE. Effect of therapeutic ionizing radiation on the human brain. Ann Neurol 2001;50:787–95.
20. Narayana A, Chang J, Thakur S, Huang W, Karimi S, Hou B, et al. Use of MR spectroscopy and functional imaging in the treatment planning of gliomas. Br J Radiol 2007;80: 347–54.
21. Kuczer D, Feussner A, Wurm R, Wust P, Michel R, Stockhammer F, et al. 123I-IMT SPECT for evaluation of the response to radiation therapy in high grade gliomas: a feasibility study. Br J Radiol 2007;80:274–8.
22. McKnight TR, von dem Bussche MH, Vigneron DB, Lu Y, Berger MS, McDermott MW, et al. Histopathological validation of a three-dimensional magnetic resonance spectroscopy index as a predictor of tumor presence. J Neurosurg 2002;97:794–802.
23. Croteau D, Scarpace L, Hearshen D, Gutierrez J, Fisher JL, Rock JP, et al. Correlation between magnetic resonance spectroscopy imaging and image-guided biopsies: semiquantitative and qualitative histopathological analyses of patients with untreated glioma. Neurosurgery 2001;49:823–9.
24. Price SJ, Jena R, Burnet NG, Hutchinson PJ, Dean AF, Peña A, et al. Improved delineation of glioma margins and regions of infiltration with the use of diffusion tensor imaging: an image-guided biopsy study. AJNR Am J Neuroradiol 2006; 27:1969–74.
25. Park I, Tamai G, Lee MC, Chuang CF, Chang SM, Berger MS, et al. Patterns of recurrence analysis in newly diagnosed glioblastoma multiforme after three-dimensional conformal radiation therapy with respect to pre-radiation therapy magnetic resonance spectroscopic findings. Int J Radiat Oncol Biol Phys 2007;69:381–9.

26. Laprie A, Catalaa I, Cassol E, McKnight TR, Berchery D, Marre D, et al. Proton magnetic resonance spectroscopic imaging in newly diagnosed glioblastoma: predictive value for the site of postradiotherapy relapse in a prospective longitudinal study. Int J Radiat Oncol Biol Phys 2008;70:773–81.
27. Krishnan AP, Asher IM, Davis D, Okunieff P, O'Dell WG. Evidence that MR diffusion tensor imaging (tractography) predicts the natural history of regional progression in patients irradiated conformally for primary brain tumors. Int J Radiat Oncol Biol Phys 2008;71:1553–62.
28. Kracht LW, Miletic H, Busch S, Jacobs AH, Voges J, Hoevels M, et al. Delineation of brain tumor extent with [11C]L-methionine positron emission tomography: local comparison with stereotactic histopathology. Clin Cancer Res 2004;10:7163–70.
29. Lee IH, Piert M, Gomez-Hassan D, Junck L, Rogers L, Hayman J, et al. Association of 11C-methionine PET uptake with site of failure after concurrent temozolomide and radiation for primary glioblastoma multiforme. Int J Radiat Oncol Biol Phys 2009;73:479–85.
30. Kelly PJ, Daumas-Duport C, Scheithauer BW, Kall BA, Kispert DB. Stereotactic histologic correlations of computed tomography- and magnetic resonance imaging-defined abnormalities in patients with glial neoplasms. Mayo Clin Proc 1987;62:450–9.
31. Halperin EC, Bentel G, Heinz ER, Burger PC. Radiation therapy treatment planning in supratentorial glioblastoma multiforme: an analysis based on post mortem topographic anatomy with CT correlations. Int J Radiat Oncol Biol Phys 1989;17:1347–50.
32. Stadlbauer A, Moser E, Gruber S, Buslei R, Nimsky C, Fahlbusch R, et al. Improved delineation of brain tumours: an automated method for segmentation based on pathologic changes of 1H-MRSI metabolites in gliomas. Neuroimage 2004;23:454–61.
33. Ganslandt O, Stadlbauer A, Fahlbusch R, Kamada K, Buslei R, Blumcke I, et al. Proton magnetic resonance spectroscopic imaging integrated into image-guided surgery: correlation to standard magnetic resonance imaging and tumour cell density. Neurosurgery 2005;56:291–8.
34. Pennington C, Kilbride L, Grant R, Wardlaw JM. A pilot study of brain tumour growth between radiotherapy planning and delivery. Clin Oncol (R Coll Radiol) 2006;18:104–8.
35. Tsien C, Gomez-Hassan D, Ten Haken RK, Tatro D, Junck L, Chenevert TL, et al. Evaluating changes in tumour volume using magnetic resonance imaging during the course of radiotherapy treatment of high-grade gliomas: implications for conformal dose-escalation studies. Int J Radiat Oncol Biol Phys 2005;62:328–32.